Variance Analysis of γ-Aminobutyric Acid (GABA)-ergic Inhibitory Postsynaptic Currents from Melanotropes of *Xenopus laevis*

J. G. G. Borst,* K. S. Kits,* and M. Bier‡

*Neurophysiology and Behavioral Physiology Unit, Department of Biology, Vrije Universiteit, 1081 HV Amsterdam, The Netherlands; ‡Section of Plastic and Reconstructive Surgery, Department of Surgery, University of Chicago, Chicago, Illinois 60637 USA

ABSTRACT We have studied the variance in the decay of large spontaneous γ-aminobutyric acid (GABA)-ergic inhibitory postsynaptic currents (IPSCs) in melanotropes of *Xenopus laevis* to obtain information about the number of $GABA_A$ receptor channels that bind GABA during the IPSCs. The average decay of the IPSCs is well described by the sum of two exponential functions. This suggests that a three-state Markov model is sufficient to describe the decay phase, with one of the three states being an absorbing state, entered when GABA dissociates from the $GABA_A$ receptor. We have compared the variance in the decay of large spontaneous IPSCs with the variance calculated for two different three-state models: a model with one open state, one closed state, and one absorbing state (I), and a model with two open states and one absorbing state (II). The data were better described by the more efficient model II. This suggests that the efficacy of GABA at synaptic $GABA_A$ receptor channels is high and that only a small number of channels are involved in generating the GABA-ergic IPSCs.

INTRODUCTION

The melanotropes in the intermediate lobe of the pituitary gland of *Xenopus laevis* are innervated by fibers from the hypothalamus that contain, among others, the neurotransmitter γ-aminobutyric acid (GABA) (De Rijk et al., 1992). This GABA-ergic innervation plays an important role in inhibiting the secretion of melanocyte-stimulating hormone (α-MSH) when a clawed toad is placed on a background that is lighter than its skin color (Verburg-van Kemenade et al., 1986). In in situ whole-cell recordings from melanotropes, inhibitory postsynaptic currents (IPSCs) have been recorded, which resulted from the opening of a single class of $GABA_A$ receptors (Borst et al., 1994). These IPSCs had a fast rise time and a much slower, bi-exponential decay, which was not dependent on the amplitude of the IPSCs. The amplitudes were very variable, but, in general, the number of channels open at the peak of the IPSCs was one to three orders of magnitude smaller than reported for end plate currents (Katz and Miledi, 1972; Anderson and Stevens, 1973). There are two possible explanations for this difference. One is that the number of channels that bind neurotransmitter is simply much smaller than in the end plate currents. Alternatively, the efficacy of the transmitter, which is directly related to the probability of opening after binding of neurotransmitter, may be much lower for the $GABA_A$ receptor channels than for the nicotinic receptor channels. In that case it is possible that in the GABA-ergic IPSCs and in the end plate currents a similar number of channels bind neurotransmitter but that the peak amplitudes of the GABA-ergic IPSCs are much lower because the $GABA_A$ receptor channels open only a small percentage of the time that GABA is bound. A low efficacy is of interest because this contributes significantly to the variability of postsynaptic currents (Faber et al., 1992; Kullman, 1993).

The decay of postsynaptic currents mediated by ligand-gated ion channels is generally thought to result from the kinetic properties of the ion channels involved (Anderson and Stevens, 1973; Dudel et al., 1980; Lester et al., 1990; Hestrin et al., 1990). The GABA-ergic IPSCs in melanotropes are probably not an exception to this rule and rebinding of neurotransmitter during the decay phase or desensitization of the receptor channels does not seem to play a role in determining the time course of the IPSCs (Borst et al., 1994). This means that by studying the decay of postsynaptic currents, it is possible to obtain information about the underlying channels. Robinson et al. (1991) have used nonstationary variance analysis (Sigworth, 1980) to study the single channel amplitude and the number of synaptic receptor channels in the decay phase of spontaneous GABA-ergic and glutamatergic postsynaptic currents. Their method does not seem suitable for studying the efficacy of GABA in melanotropes. As discussed by the authors, the estimate of the number of receptors obtained with their method is not very reliable. Moreover, for their method to be applicable to the analysis of spontaneous postsynaptic currents, the number of postsynaptic receptors must be the same in all active synapses on a cell. However, it is unlikely that this holds true in the case of the melanotropes of *X. laevis* (Borst et al., 1994). We have used an alternative approach to obtain an estimate for the number of channels that are involved in the decay of the IPSCs.

Received for publication 25 August 1993 and in final form 4 April 1994.

Address reprint requests to Dr. K. S. Kits, Neurophysiology and Behavioral Physiology Unit, Department of Biology, Vrije Universiteit, De Boelelaan 1087, 1081 HV Amsterdam, The Netherlands. Tel.: 31-20-548-2992; Fax: 31-20-642-9202.

0006-3495/94/07/183/07 $2.00

THEORY

The decay of the IPSCs is adequately described by the sum of two exponential functions (Borst et al., 1994; see also Fig. 1).

$$X(t) = A_1 e^{-\lambda_1 t} + A_2 e^{-\lambda_2 t} \quad (1)$$

The time course of small IPSCs is not different from large IPSCs (Borst et al., 1994). It is likely that the $GABA_A$ receptor channels have a single conductance level and that rebinding of neurotransmitter does not play a role during the decay phase (Borst et al., 1994). Under these assumptions the decay of the IPSCs is logically equivalent to the following three-state Markov scheme:

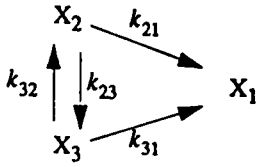

(2)

where X_2 and X_3 are agonist-bound and X_1 is the absorbing closed state, which is entered when GABA unbinds from the $GABA_A$ receptor channels. Two possible schemes can be discriminated: I. Only one of the agonist-bound states is open. Because of the symmetry in the scheme we can, without loss of generality, take this to be X_3. II. Both agonist-bound states, X_2 and X_3, are open states. This scheme does not contain agonist-bound closed states, all channels that participate in the decay are open until they lose the GABA. In this case the efficacy of GABA is the highest possible.

Note that the sequential schemes

$$C_1 \rightleftharpoons C_2 \rightleftharpoons O_3 \qquad \text{and} \qquad C_1 \rightleftharpoons O_2 \rightleftharpoons C_3$$

are special cases of scheme I and that

$$C_1 \rightleftharpoons O_2 \rightleftharpoons O_3$$

is a special case of scheme II. In addition, more complex schemes, with four or more states, may reduce to one of the two schemes if the time spent in one or more of the states is negligible.

Our strategy will be to intercept the IPSCs late in the decay at a fixed amplitude and calculate the variance around the average of the rest of the decay. Because at the interception point the contribution of the fast exponential function can be neglected, it becomes possible to calculate the theoretical variance for the two different theoretical models as well. The variance for the model with a single open state (model I) is clearly larger than the variance for the model with two open states (model II), since in model I more channels participate in the decay than in model II. In the later sections of this paper, we will test which model gives the best description of the spontaneous IPSCs in the intermediate lobe of the pituitary gland of *X. laevis*.

For the kinetic scheme of Eq. 2 the time evolution of the averages in states 2 and 3 is determined by

$$\begin{pmatrix} \dot{x}_2 \\ \dot{x}_3 \end{pmatrix} = \begin{pmatrix} -(k_{21} + k_{23}) & k_{32} \\ k_{23} & -(k_{32} + k_{31}) \end{pmatrix} \begin{pmatrix} x_2 \\ x_3 \end{pmatrix}. \tag{3}$$

With the initial conditions $X_2(0) = N$ and $X_3(0) = M$ we obtain for the solution of Eq. 3

$$\begin{aligned} x_2(t) = \frac{1}{\lambda_1 - \lambda_2} [\{N(\lambda_1 - k_{32} - k_{31}) - Mk_{32}\}e^{-\lambda_1 t} \\ + \{-N(\lambda_2 - k_{32} - k_{31}) + Mk_{32}\}e^{-\lambda_2 t}] \\ x_3(t) = \frac{1}{\lambda_1 - \lambda_2} [\{M(\lambda_1 - k_{21} - k_{23}) - Nk_{23}\}e^{-\lambda_1 t} \\ + \{-M(\lambda_2 - k_{21} - k_{23}) + Nk_{23}\}e^{-\lambda_2 t}] \end{aligned} \tag{4}$$

where λ_1 and λ_2 are the eigenvalues of the matrix in Eq. 3. They have the form

$$\begin{aligned} \lambda_{1,2} = \{(k_{21} + k_{23} + k_{32} + k_{31}) \pm \sqrt{((k_{21} + k_{23} + k_{32} + k_{31})^2 \\ - 4(k_{21}k_{32} + k_{21}k_{31} + k_{23}k_{31}))}\}/2 \end{aligned} \tag{5}$$

with

$$\begin{aligned} \lambda_1 + \lambda_2 &= k_{21} + k_{23} + k_{32} + k_{31} \\ \lambda_1\lambda_2 &= k_{21}k_{32} + k_{21}k_{31} + k_{23}k_{31}. \end{aligned} \tag{6}$$

As a convention we take $\lambda_1 > \lambda_2$.

It is not possible to distinguish between model I and II on just the basis of decay phase averages and we have to turn to the second moment, the variance, to make the discrimination.

The quantity $C = A_1/(A_1 + A_2)$ is related to a ratio $\rho = X_2(0)/X_3(0) = N/M$, i.e., the distribution of the channels over X_2 and X_3 at the peak of the IPSC. This ρ is a consequence of rise phase dynamics and is unknown. We therefore start the variance analysis at a fixed amplitude in the tail of the IPSCs, at a point where the further decay is dominated by the slower time constant. In the tail both $X_2(t)$ and $X_3(t)$ decay exponentially (with exponent $-\lambda_2$) and in the calculations the fact that for monoexponential decay the variance equals the average can be used.

Variance for model II

Suppose we have 1 open channel at a "$t = 0$" in the tail. Let $p(t)$ be the probability that the channel is still open at time t. We have

$$p(t) = e^{-\lambda_2 t} \tag{7}$$

and for the variance

$$\sigma_1^2(t) = p(t) - (p(t))^2 = e^{-\lambda_2 t} - (e^{-\lambda_2 t})^2. \tag{8}$$

For k_0 open channels, instead of a single open channel at $t = 0$, the variances will add

$$\sigma_{k_0}^2(t) = k_0\{e^{-\lambda_2 t} - (e^{-\lambda_2 t})^2\}. \tag{9}$$

The peak of the variance is at $t = (\ln 2)/\lambda_2$, with maximum amplitude $k_0/4$.

Variance for model I

We define $P_{33}(t)$ as the probability that a channel that is in X_3 at $t = 0$ is also in X_3 at time t and $P_{23}(t)$ as the probability

that a channel that is in X_2 at $t = 0$ is in X_3 at time t. $P_{33}(t)$ can be easily evaluated by substituting $N = 0$ and $M = 1$ in the equation for $X_3(t)$ under Eq. 4

$$P_{33}(t) = \frac{1}{\lambda_1 - \lambda_2} \cdot \{(\lambda_1 - k_{21} - k_{23})e^{-\lambda_1 t} - (\lambda_2 - k_{21} - k_{23})e^{-\lambda_2 t}\}. \quad (10)$$

Similarly, by substituting $N = 1$ and $M = 0$ in the equation for $X_3(t)$ under Eq. 4 we find

$$P_{23}(t) = \frac{-k_{23}}{\lambda_1 - \lambda_2}(e^{-\lambda_1 t} - e^{-\lambda_2 t}). \quad (11)$$

The variance among the channels in the open state that were in X_3 at $t = 0$ is

$$\sigma^2_{33}(t) = MP_{33}(t)\{1 - P_{33}(t)\}. \quad (12)$$

The variance among the channels in the open state that were in X_2 at $t = 0$ is

$$\sigma^2_{23}(t) = NP_{23}(t)\{1 - P_{23}(t)\}. \quad (13)$$

Adding these two, we obtain the variance in the number of open channels for any M and N

$$\sigma^2_m(t) = \bar{m}(t) - MP^2_{33}(t) - NP^2_{23}(t). \quad (14)$$

The IPSCs will be intercepted in the tail, at a fixed amplitude. At this point only the slow component is important. From then on, the average number of open channels, $\bar{m}(t) = m_0 \exp(-\lambda_2 t)$ and the variance in the tail will be

$$\sigma^2_m(t) = m_0 e^{-\lambda_2(t)} - m_0 P^2_{33}(t) - n_0 P^2_{23}(t) \quad (15)$$

Although the number of open channels at the point of interception (m_0) will be the same for all IPSCs of an experiment, the number of closed channels at that point (n_0) may vary. Because the decay of both the number of closed and the number of open channels is exponential in the tail of IPSCs, the variance $(\Delta n_0)^2$ is equal to n_0. The standard deviation in $\Delta m(t)$ around $\bar{m}(t)$ caused by Δn_0 can be derived by substituting $n_0 \pm \Delta n_0$ in Eq. 4 and thus obtaining a $X'_3(t)$. Then

$$\Delta m(t) = x'_3(t) - x_3(t) = \frac{\Delta n_0 k_{23}}{\lambda_1 - \lambda_2}\{\mp e^{-\lambda_1 t} \pm e^{-\lambda_2 t}\} \quad (16)$$

where $X_3(t) = \bar{m}(t)$, the average number of channels in the open state at time t, a quantity that can be measured given a sufficiently large number of PSCs. From Eq. 11 this is seen to be identical to $n_0(P_{23}(t))^2$. Adding this, as a source of variance, to Eq. 15 we get

$$\sigma^2_m(t) = m_0\{e^{-\lambda_2(t)} - P^2_{33}(t)\}. \quad (17)$$

The variance in the number of open channels for model I is therefore obtained by substituting Eq. 10 in Eq. 17

$$\sigma^2_m(t) = m_0\left\{ e^{-\lambda_2 t} - \left(\frac{1}{\lambda_1 - \lambda_2}((\lambda_1 - k_{21} - k_{23})e^{-\lambda_1 t} - (\lambda_2 - k_{21} - k_{23})e^{-\lambda_2 t})\right)^2\right\}. \quad (18)$$

Note that the λ_1 component, even though it has disappeared from the formula for the average number of open channels $\bar{m}(t)$, is still present in the variance, i.e., still plays a role in how fast identical initial conditions in the tail move away from each other.

The ratio $C = A_1/(A_1 + A_2)$ from Eq. 1 can be related to parameters and initial conditions via Eqs. 4. C tells us through these formulas how agonist-bound channels are divided over X_2 and X_3 at the end of the rise phase. We obtain

$$(1 - C)\lambda_1 + C\lambda_2 = k_{21} + k_{23}(1 + \rho). \quad (19)$$

Given λ_1 and λ_2, the variance is a one parameter family of curves. The range over which $(k_{21} + k_{23})$ can be varied is very limited: in Eq. 19 we must have $\rho \geq 0$ and $0 < C < 1$. This implies

$$\lambda_2 < k_{21} + k_{23} \leq (1 - C)\lambda_1 + C\lambda_2. \quad (20)$$

The equation for the maximum variance for model I is obtained by substituting λ_2 for $k_{21} + k_{23}$ in Eq. 18

$$\sigma^2_{max}(t) = m_0\{e^{-\lambda_2 t} - (e^{-\lambda_1 t})^2\}. \quad (21)$$

The minimum variance is obtained when $k_{21} + k_{23} = (1 - C)\lambda_1 + C\lambda_2$ in Eq. 18

$$\sigma^2_{min}(t) = m_0\left\{ e^{-\lambda_2 t} - \left(\frac{1}{\lambda_1 - \lambda_2}(Ce^{-\lambda_1 t} + (1 - C)e^{-\lambda_2 t})\right)^2\right\}. \quad (22)$$

A single exponential function is not sufficient to describe the decay of the averaged experimental IPSCs, which means that C is clearly larger than 0. Since $\lambda_1 > \lambda_2$, the quadratic term in Eq. 22 will be smaller than in Eq. 9 and the variance for model I is higher than for model II (see Fig. 3, *A–C*). From Eq. 22 it can be seen that the more C lies above 0, the bigger the gap in the figure between the curve from model II and the family of curves from model I will be.

After binding of GABA, the open probability of channels that gate according to model II is 1. For channels that gate according to model I it is not possible to calculate a precise number for the open probability, since even if the variance of the currents is known, the rate constants cannot be uniquely calculated. However, it is possible to give an upper limit for the open probability. The ratio between the number of channels in the closed and the open bound state (ρ) is unknown at the peak of the IPSC. Late in the decay it will reach a steady state value ρ', which can be calculated from Eqs. 4 and 6

$$\rho' = \lim_{t\to\infty}\frac{X_2(t)}{X_3(t)} = \frac{\lambda_1 - k_{21} - k_{23}}{k_{23}}. \quad (23)$$

The open probability will be largest if $k_{21} = 0$ and $k_{23} = (1 - C)\lambda_1 + C\lambda_2$. The upper limit for the open probability is therefore

$$P_o = 1 - \frac{C(\lambda_1 - \lambda_2)}{\lambda_1}. \quad (24)$$

MATERIALS AND METHODS

Adult clawed toads (*X. laevis*) were bred at the Department of Animal Physiology of the University of Nijmegen. They were adapted to a white background for at least 3 weeks before the experiment. The size of the melanotropes is smaller in white-adapted animals (Borst et al., 1994), resulting in a higher signal to noise ratio in whole-cell recordings. The toads were placed on ice and decapitated. The neurointermediate lobe was incubated for 20 min in the extracellular buffer (see below) with 0.1% collagenase (type V, Sigma, St. Louis, MO), to facilitate the subsequent removal of connective tissue.

In situ whole-cell recordings were made as described by Edwards et al. (1989). The experiments were performed at room temperature. The recording chamber was continuously perfused (2–3 ml/min) with a buffer that consisted of (in mM): 90 NaCl, 2 KCl, 2 $CaCl_2$, 2 $MgCl_2$, 10 D-glucose, 26 $NaHCO_3$. The pH was kept at 7.4 by bubbling the solution with carbogen (95% O_2, 5% CO_2). The pipette (intracellular) solution consisted of (in mM): 100 CsCl, 0.2 MgATP, 1.8 $MgCl_2$, 2 $CaCl_2$, 10 EGTA, 10 HEPES (pH adjusted to 7.4 with CsOH). Pipettes were pulled on a Flaming/Brown P-87 puller (Sutter Instruments, Novato, CA) from thick-walled borosilicate glass (Clark GC150-10, Reading, England, 5 MΩ). They were coated with Sylgard (Dow Corning, Seneffe, Belgium). Whole-cell recordings were made with an EPC-7 patch-clamp amplifier (List, Darmstadt, Germany). The holding potential was −80 mV. Three experiments were selected that contained a large number of large IPSCs. In these experiments, errors in the holding potential as a result of series resistance were <7 mV. The product of series resistance and membrane capacitance was <70 μs. The average amplitude of the IPSCs was constant during the experiment.

Current recordings were stored on a DAT-tape recorder (16-bit, DC to 44 KHz). They were filtered at 1 kHz (−3dB, 8-pole Bessel filter) and when the currents exceeded a threshold level of 150 or 200 pA, a period of 400 ms was digitized at 200 μs per point (CED1401 12-bit A/D converter, Cambridge Electronic Design, Cambridge, UK). For further analysis, traces were selected that had stable baselines and contained only a single IPSC.

For the determination of the average time course, the IPSCs were aligned by minimizing the difference between the 20–80% rise times of the IPSCs and averaged. Using a χ^2 criterion and a Levenberg-Marquardt algorithm, one or the sum of two exponential functions were fitted to the decay of the averaged IPSCs.

For each IPSC the point in the decay was found where the currents crossed a certain fixed level. This was the starting point ($t = 0$) for the variance analysis. For each experiment, this level was chosen sufficiently high to obtain enough open channels for the variance analysis, but also sufficiently low to make it possible to neglect the contribution of the fast exponential decay to the further decay of the synaptic currents. At the height of the levels used in the decay analysis, the average contribution of the fast exponential decay was 2–4%. If the level was crossed more than once (e.g., Fig. 2 *A*), one of these crossings was randomly chosen. This way a population of currents which all started at the same level, but decayed differently, was obtained. Mean and variance of this population were calculated.

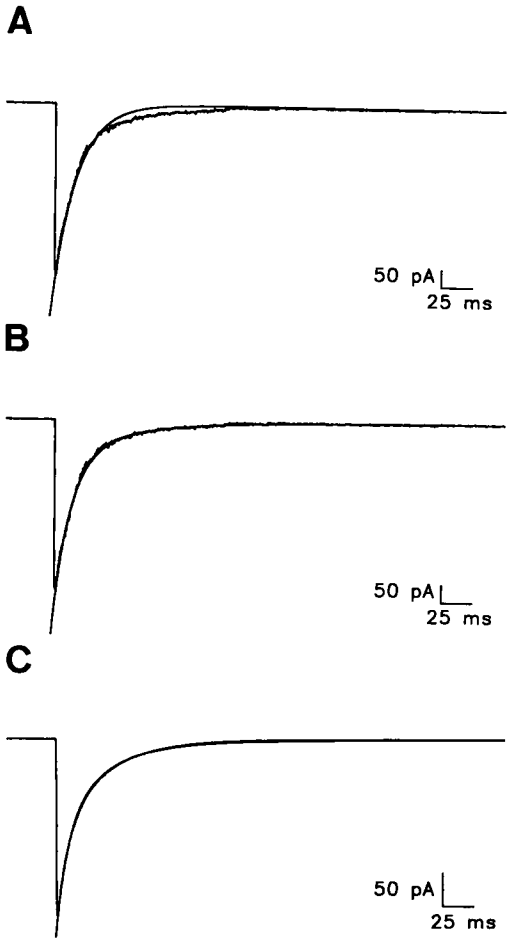

FIGURE 1 Decay of spontaneous GABA-ergic IPSCs. Inward current, corresponding to outward movement of Cl^- ions, is downward. (*A*) Fit of the decay of an IPSC with a single exponential function with a time constant of 19.0 ms. (*B*) Fit with the sum of two exponential functions with time constants of 14.2 and 59.4 ms. The contribution of the fast time constant to the peak amplitude was 80.2%. (*C*) Fit of the averaged IPSCs from the same experiment with the sum of two exponential functions with time constants of 10.3 and 39.7 ms. The peak contribution of the fast time constant was 52.1%.

RESULTS

Time course

In whole-cell recordings, the melanotropes received spontaneous GABA-ergic inputs. The amplitudes of the IPSCs were very variable, both IPSCs with a peak amplitude of <10 pA and IPSCs >400 pA were observed. The time course of the largest IPSCs was analyzed in detail in three cells from three different clawed toads.

The IPSCs had a fast rise time. The rise times of the averaged IPSC were <1 ms. The decays were much slower. In almost all IPSCs, the fit of the decay with a single exponential function contained a systematic error (Fig. 1 *A*), but the decay was well described by the sum of two exponential functions (Fig. 1 *B*). The decay of the averaged IPSCs was also well described by the sum of two exponential functions (Fig. 1 *C*). The fast time constant was 10.2 ± 1.2 ms (SD). The slow time constant was 34.4 ± 5.3 ms. The contribution of the fast time constant to the peak amplitude was 57.9 ± 4.2%. However, there was also a very slow, third component, that contributed only about 1% to the peak amplitude and resulted from a number of very slowly decaying IPSCs. The decay of the IPSCs became slower with time, mostly during the first few minutes after establishing the whole-cell configuration. During the period used for the variance analysis (10–20 min), the decay time increased around 25%. This was not due to an increase in the series resistance, since rise times remained fast throughout the same period.

The good signal-to-noise ratio made it possible to discriminate $GABA_A$ receptor channels in the decay phase (Fig. 2 *A*). The amplitude of these channels was estimated

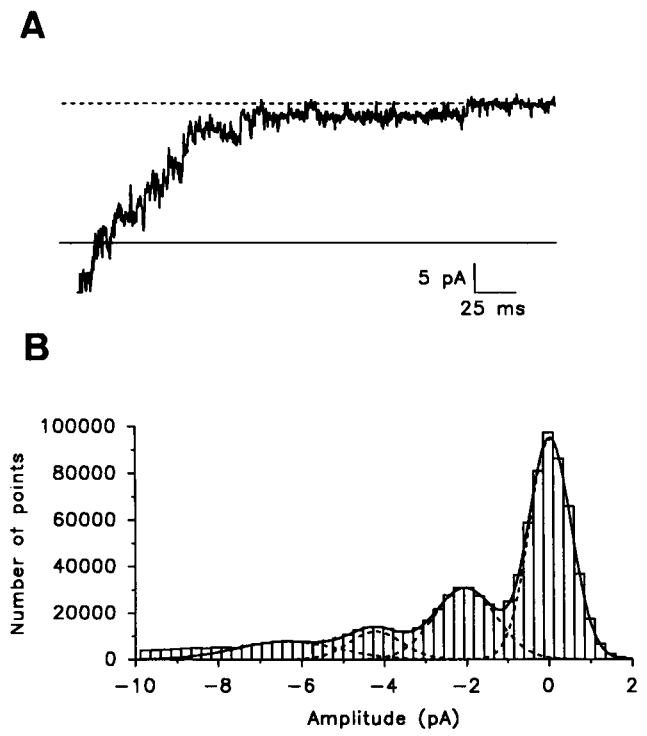

FIGURE 2 (*A*) Magnified tail of the same IPSC as shown in Fig. 1, *A* and *B*. The solid horizontal line is at the amplitude at which the IPSCs were intercepted (−24 pA), the dotted line is at the baseline level. (*B*) All-points histogram of >200 large spontaneous IPSCs. The largest peak is at the baseline level, the other peaks are at 1–3 open $GABA_A$ receptor channels. Also shown is the fit with the sum of 4 Gaussians. Average peak distance was 2.137 pA.

from fits of the sum of 3–4 Gaussians to all-points histograms of the IPSCs (Fig. 2 *B*). On average it was -2.12 ± 0.04 pA. Although the individual $GABA_A$ receptor channels displayed bursting behavior (Fig. 2 *A*), large increases in the amplitudes of the IPSCs during the decay phase were generally not observed (Figs. 1 *A* and 2 *A*).

Variance analysis

The IPSCs were intercepted at a fixed level, as described in Materials and Methods. The variance of the currents starting from the point of interception was calculated. This variance is 0 at the interception point ($t = 0$), since all IPSCs were intercepted at the same amplitude. It then rises to a maximum, as the amplitudes of the different IPSCs diverge and returns to 0 as the IPSCs decay to the baseline level. The variance against time plot is shown for the three experiments in Fig. 3. In the same figure the expected variance for the two theoretical models, calculated as described in the Theory section, is shown. The peak of the experimentally obtained variance fell later than the peak of the variance of model I and the amplitude was clearly lower. However, the increase in the experimental variance after the point of interception was faster than for model II and the peak was somewhat higher than the peak of the model II variance. The variance against time differed from both theoretical models in that the return to the baseline level was clearly slower than in model I or II. However, the return of the average intercepted current to the baseline level was also slower than predicted by the fit of the averaged IPSC (Fig. 3 *D*).

DISCUSSION

In whole-cell recordings in the intermediate lobe of the pituitary gland of *X. laevis*, spontaneous IPSCs were observed that had a variable amplitude, a fast rise time, and a bi-exponential decay. In the tails of the IPSCs, a single class of $GABA_A$ receptor channels was observed.

The good description of both the individual and the averaged IPSCs with the sum of two exponential functions suggests that a three-state model is sufficient to describe the behavior of the $GABA_A$ receptor channels during the decay phase of the IPSCs, with one of the three states being a closed absorbing state. Of the other two states, at least one must be an open state. This leaves two possible models. For the model with two open states (model II) the efficacy of GABA will be the highest possible, since the probability of opening of the $GABA_A$ receptor channels in the IPSCs, after binding of GABA, would be 1. The probability of opening for channels that gate according to model I will be lower. An upper limit for the open probability, given the observed values for C, λ_1 and λ_2, would be ~0.6 (Eq. 24). This value would only be reached if all channels that had still bound GABA at the point of interception would open before losing the GABA, otherwise it would be lower.

Because the efficacy of GABA is lower in model I than in model II, the variance in the decay of the postsynaptic currents is higher for model I. The variance has been calculated for both models in the Theory section. The variance from the recorded IPSCs was best described by model II, since the peak of even the minimum variance model I was clearly higher and fell earlier than the peak of the variance from the IPSCs. Therefore we conclude that model I, which contains an agonist-bound closed state, does not give a good description of the experimental data. However, the description of the experimental variance by model II was also not perfect. The experimental variance had a faster rise phase, a higher peak, and returned to the baseline level slower than the curve from model II. We have simulated the decay of IPSCs (Robertson et al., 1991) using the two theoretical models. The parameters were taken as much as possible from one of the experiments; this included the baseline noise, the amplitudes of the IPSCs, and the estimated contribution of the two exponential functions to the peak amplitudes. The results of these simulations showed that the presence of variations in peak amplitude, variations in the contribution of the two exponents to the peak amplitude, variations in the contribution of the fast exponent at the interception point, and the presence of baseline noise introduced a total error of <5% (data not shown).

Three other factors are probably more relevant for the observed differences between the variance in the experimental data and in model II. One is that the average decay became

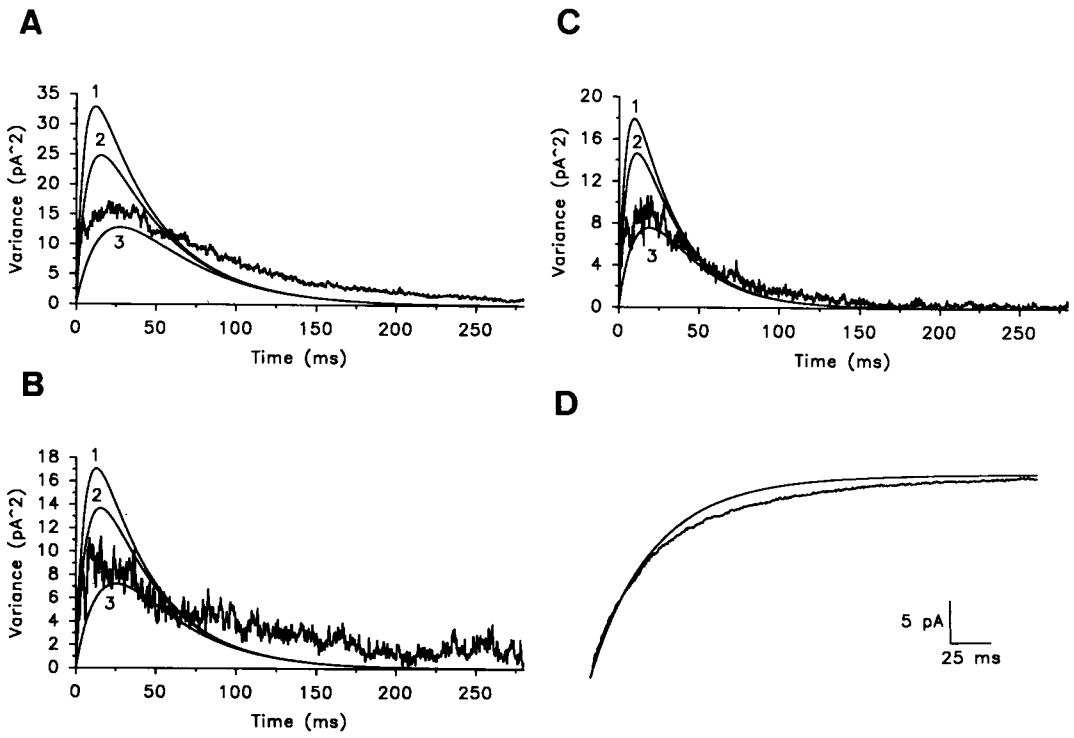

FIGURE 3 (*A–C*) Variance of the decay of the GABA-ergic IPSCs in three experiments. The results of the experiment shown in *A* were also used for Fig. 1. The $t = 0$ point is the point in time at which the IPSCs were intercepted. In each case the noisy trace was obtained from the IPSCs. The number 1 denotes the maximum possible variance for model I, number 2 denotes the minimum variance for model I, and number 3 denotes the variance for model II. These curves were calculated according to Eqs. 9, 25, and 26 in the Theory section. The parameters used in these calculations for the experiments shown in *A*, *B* and *C*, were, respectively: $GABA_A$ receptor channel amplitude 2.137, 2.06, and 2.164 pA; interception amplitude −24, −14, and −14 pA; *C* was 0.521, 0.595, and 0.621; λ_1 ($=1/\tau_1$) 97.1, 85.7, and 114.8 s^{-1}; λ_2 25.2, 27.6, and 36.9 s^{-1}. The numbers of IPSCs used for the calculation of the variance were 233, 53, and 73. The baseline variance, which was estimated from the current immediately preceding the IPSCs, was subtracted from the calculated variance. The baseline variance was 0.43, 0.90, and 0.68 pA^2 in *A*, *B* and *C*, respectively. (*D*) Mean of the intercepted IPSCs of which the variance has been calculated in *A*. The solid line is the expected decay, with a time constant of 39.7 ms, obtained from the fit with two exponential functions of the averaged IPSC.

slower during the experiment, as judged from fits on the individual IPSCs. This will increase the variance and slow the return of the amplitude of the variance to the baseline level. A second cause was the occurrence of IPSCs with very slow decays. These resulted in a slow, third component in the averaged IPSCs which would contribute only little to the peak amplitude, but which was more important in the tails of the decay. A third cause for the extra variance in the experimental data as compared with the variance of model II is the presence of fast intraburst closures (Fig. 2 *A*). We have measured the probability of opening of $GABA_A$ receptor channels in the decay of IPSCs in recordings with very low baseline noise. In general, the open probability was high (J. Borst, J. Lodder, and K. Kits, unpublished observations). In outside-out patches from cultured neurons, a high probability of opening during bursts of single $GABA_A$ receptor channels has also been observed in the presence of high concentrations of GABA (Newland et al., 1991).

Despite these three causes, which all three increase the measured variance, the peak variance was only slightly higher than the variance from model II. The latter is the lowest possible for postsynaptic currents with a bi-exponential decay. Such a low peak variance occurs when the GABA channels open as soon as GABA binds and remain open until GABA unbinds. Since the variance calculated from the spontaneous IPSCs in the melanotropes was only slightly higher than for model II, we conclude that the efficacy of GABA at the synaptic $GABA_A$ receptor channels in melanotropes is high. This is in agreement with a single-channel study in which the efficacy was also estimated to be rather high (Bormann and Clapham, 1985), although not as high as the efficacy of acetylcholine for nicotinic receptor channels (Ogden and Colquhoun, 1983; Colquhoun and Sakmann, 1985; Sine and Steinbach, 1986; Dilger and Brett, 1990).

Although model II provides an adequate description of the kinetics of the $GABA_A$ receptor channels during the decay of the IPSCs, it clearly does not do justice to the complex gating that has been observed in single-channel recordings (MacDonald et al., 1989; Newland et al., 1991). However, it should be noted that, in general, more complicated schemes with two open states will reduce to model II if the channels spend very little time in the ligand-bound closed states. For example, a scheme with three closed and two open states was used by Busch and Sakmann (1990) to simulate IPSCs with a fast rise time and a bi-exponential decay. The rate constants chosen by them were such that, for the decay, this scheme can be reduced to model II.

The high efficacy of GABA for the $GABA_A$ receptor channels would imply that during the peak of the IPSC almost all ligand-bound channels are open and, apart from the fast intraburst closures, they remain open until GABA dissociates from the channels. This conclusion is supported by the (qualitative) observation that large increases of the currents during the decay of the IPSCs were generally not seen. It means that the gating of the channels that have bound neurotransmitter is not a major cause (cf. Faber et al., 1992) for the observed variability in the peak amplitudes of the spontaneous currents in the melanotropes (Borst et al., 1984). The high efficacy implies that in many IPSCs less than twenty $GABA_A$ receptor channels bind GABA. However, the method of variance analysis presented here is not suitable to estimate the total number of channels that can bind GABA (i.e., the number of available channels; see Sigworth, 1980). It is possible that in most spontaneous IPSCs, the number of channels that bind GABA represents only a small fraction of the number of available channels, for example if the amount of GABA that is released is limiting. However, differences in the number of postsynaptic channels between synapses are probably a much more important cause for the variability in the peak amplitudes of the spontaneous IPSCs (Borst et al., 1994).

We thank J. C. Lodder for technical assistance and Prof. Dr. F. H. Lopes da Silva for reading an earlier version of the manuscript.

J. G. G. B. was supported by grant 426.903-P from the Foundation for Fundamental Biological Research (BION). M.B. was supported by a travel grant from the Netherlands Organization for the Advancement of Research (NWO).

REFERENCES

Anderson, C. R., and C. F. Stevens. 1973. Voltage clamp analysis of acetylcholine produced end-plate current fluctuations at frog neuromuscular junctions. *J. Physiol.* 235:665–691.

Bormann, J., and D. E. Clapham. 1985. γ-Aminobutyric acid receptor channels in adrenal chromaffin cells: a patch clamp study. *Proc. Natl. Acad. Sci. USA.* 82:2168–2172.

Borst, J. G. G., J. L. Lodder, and K. S. Kits. 1994. Large amplitude variability of GABA-ergic IPSCs in melanotropes from *Xenopus laevis*: evidence that quantal size differs between synapses. *J. Neurophysiol.* 71: 639–655.

Busch, C., and B. Sakmann. 1990. Synaptic transmission in hippocampal neurons: numerical reconstruction of quantal IPSCs. *Cold Spring Harbor Symp. Quant. Biol.* 55:69–80.

Colquhoun, D., and B. Sakmann. 1985. Fast events in single-channel currents activated by acetylcholine and its analogues at the frog muscle end-plate. *J. Physiol.* 369:501–557.

de Rijk, E. P. C. T., F. J. C. van Strien, and E. W. Roubos. 1992. Demonstration of coexisting catecholamine (dopamine), amino acid (GABA) and peptide (NPY) involved in inhibition of melanotrope cell activity in *Xenopus laevis*. *J. Neurosci.* 12:864–871.

Dilger, J. P., and R. S. Brett. 1990. Direct measurement of the concentration and time-dependent open probability of the nicotinic acetylcholine receptor channel. *Biophys. J.* 57:723–731.

Dudel, J., W. Finger, and H. Stettmeier. 1980. Inhibitory synaptic channels activated by γ-aminobutyric acid (GABA) in crayfish muscle. *Pfluegers Arch.* 387:143–151.

Edwards, F. A., A. Konnerth, B. Sakmann, and T. Takahashi. 1989. A thin slice preparation for patch clamp recordings from neurones of the mammalian central nervous system. *Pfluegers Arch.* 414:600–612.

Faber, D. S., W. S. Young, P. Legendre, and H. Korn. 1992. Intrinsic quantal variability due to stochastic properties of receptor-transmitted interactions. *Science.* 258:1494–1498.

Hestrin, S., P. Sah, and R. A. Nicoll. 1990. Mechanisms generating the time course of dual component excitatory synaptic currents recorded in hippocampal slices. *Neuron.* 5:247–253.

Katz, B., and R. Miledi. 1972. The statistical nature of the acetylcholine potential and its molecular components. *J. Physiol.* 224:665–699.

Kullman, D. M. 1993. Quantal variability of excitatory transmission in the hippocampus: implications for the opening probability of fast glutamate-gated channels. *Proc. R. Soc. Lond.* 253: 107–116.

Lester, R. A. J., J. D. Clements, G. L. Westbrook, and C. E. Jahr. 1990. Channel kinetics determine the time course of NMDA-receptor mediated synaptic currents. *Nature.* 346:565–567.

MacDonald, R. L., C. J. Rogers, and R. E. Twyman. 1989. Kinetic properties of the $GABA_A$ receptor main conductance state of mouse spinal cord neurones in culture. *J. Physiol.* 410:479–499.

Newland, C. F., D. Colquhoun, and S. G. Cull-Candy. 1991. Single channels activated by high concentrations of GABA in superior cervical ganglion neurones of the rat. *J. Physiol.* 432:203–233.

Ogden, D. C., and D. Colquhoun. 1983. The efficacy of agonists at the frog neuromuscular junction studied with single channel recording. *Pfluegers Arch.* 399:246–248.

Robinson, H. P. C., Y. Sahara, and N. Kawai. 1991. Nonstationary fluctuation analysis and direct resolution of single channel currents at postsynaptic sites. *Biophys. J.* 59:295–304.

Sigworth, F. J. 1980. The variance of sodium current fluctuations at the node of Ranvier. *J. Physiol.* 307:97–129.

Sine, S. M. and J. H. Steinbach. 1986. Activation of acetylcholine receptors on clonal mammalian B3H-1 cells by low concentrations of agonist. *J. Physiol.* 373:129–162.

Verburg-van Kemenade, B. M. L., M. Tappaz, L. Paut, and B. G. Jenks. 1986. GABAergic regulation of melanocyte-stimulating hormone secretion from the pars intermedia of *Xenopus laevis*: immunocytochemical and physiological evidence. *Endocrinology.* 118:260–267.